A HIGHLY EFFICIENT ENGINEERING TOOL FOR THREE-DIMENSIONAL SCRAMJET FLOWFIELD AND HEAT TRANSFER COMPUTATIONS

Pradeep S. Kamath
Analytical Services and Materials Inc.
Hampton, Virginia

Richard W. Hawkins
Analytical Services and Materials Inc.
Hampton, Virginia

Nathaniel R. Baker
Lockheed Engineering and Sciences Company
Hampton, Virginia

Charles R. McClinton
NASA Langley Research Center
Hampton, Virginia

ABSTRACT

The SIMPLE-based parabolic flow code, SHIP3D has been under development for use as a parametric design and analysis tool for scramjets. This paper demonstrates some capabilities and applications of the code and is also a report on its current status. The focus is on the combustor for which the code has been mostly used. Recently, it has also been applied to nozzle flows. Code validation results are presented for combustor unit problems involving film cooling and transverse fuel injection, and for a nozzle test. A parametric study of a film cooled or transpiration cooled Mach 16 combustor is also conducted to illustrate the application of the code to a design problem.

INTRODUCTION

There is currently great interest in the development of computer codes to predict the performance of hypersonic, air-breathing propulsion systems at flight speeds that are beyond ground test capabilities. Of particular interest among air-breathing power plants for hypersonic flight is the hydrogen-fueled, airframe-integrated scramjet, a schematic sketch of which is shown in Figure 1. In this
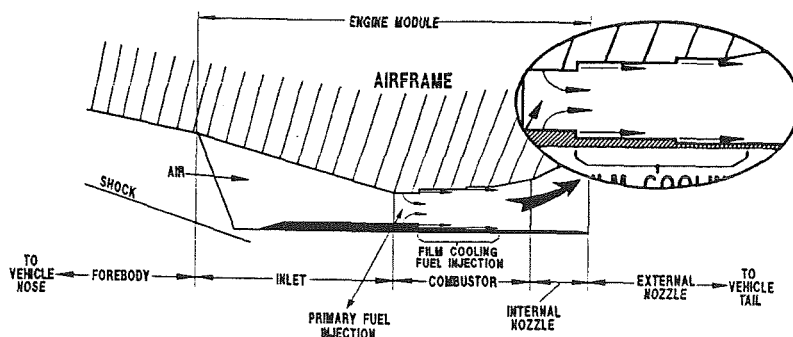

Figure 1. Schematic of Airframe-Integrated Scramjet

design, modular engines mounted on the lower surface of the fuselage process most of the compressed air mass contained within the envelope of the vehicle forebody bow shock [1]. Each module is a duct of rectangular cross-section consisting of an inlet, a combustor and an internal nozzle. The exhaust from these engines expands against and pressurizes the rear end of the vehicle, thus generating thrust.

The performance of these engines have heretofore been analyzed using one-dimensional cycle codes into which are empirically incorporated, most of the knowledge gained of the individual components in the propulsion flowpath, by testing at low Mach numbers. Although CFD has recently been used to analyze portions of the propulsion flowpath in greater detail [2], the overall vehicle performance is still computed using cycle codes. It has become clear that even this limited use of CFD involves an expense that borders on being prohibitive. This is particularly true for the combustor where the conventional solution method of time-marching the Navier-Stokes equations to convergence requires in excess of one hundred Cray-2 CPU hours, on a grid just fine enough to get an adequate estimate of the combustion efficiency but not of heat transfer and skin friction.

The need to bridge the gap between these two approaches is critical if CFD is to be used for design and parametric studies. Key to achieving this is to use methods that fully exploit the efficiencies inherent in these flows, one of which is the largely parabolic nature of the flow over most of the propulsion flowpath at hypersonic speeds. Thus, one approach is to treat locally elliptic regions in a parabolic manner while ensuring the global conservation of mass, momentum and energy. In the combustor, this mainly requires the parabolic treatment of fuel injection since regions of elliptic flow are usually around the injectors. Depending on its design, a primary fuel injector may be, a discrete hole flush with the wall for sonic, transverse injection, or a ramped strut or wedge-shaped protrusion into the flow for supersonic, parallel injection. A parallel injection slot is also placed at the bottom of a backward-facing step at one or more axial stations on each wall for film cooling. In addition, portions of the combustor wall may be transpiration cooled with fuel.

The topic of the first portion of the paper is film cooling. The methodology for the parabolic computation of parallel injection from a step is outlined and validated for a classic, hydrogen-cooled combustor film cooling case. Next follows a similar discussion on transverse injection and its validation against mixing data. The practical use of these capabilities is then demonstrated by a parametric analysis of a conceptual combustor with transverse fuel injection and film cooling or transpiration cooling. The parabolic treatment of fuel injection from ramp and strut injectors that protrude into the flow is currently under development and is not discussed here. Finally, a nozzle computation and comparison with test data is shown.

FILM COOLING

Film cooling in a scramjet combustor involves the injection of a portion of the hydrogen fuel parallel to and alongside the planar walls of the combustor to lower the heat load on the wall. Ignoring regenerative cooling and the effect of film cooling on engine performance, which are discussed in the parametric study later in the paper, the task reduces to the computation of the wall heat flux and shear stress in a turbulent, reacting flow. A representative unit problem is shown in Figure 2, which is a schematic of a test conducted in the Calspan 48-inch shock tunnel. The bottom wall of the model represents the body side of the vehicle and the top wall, the cowl side (see Figure 1). Both walls are film cooled in the test, with 59 percent of the fuel used on the bottom wall and 41
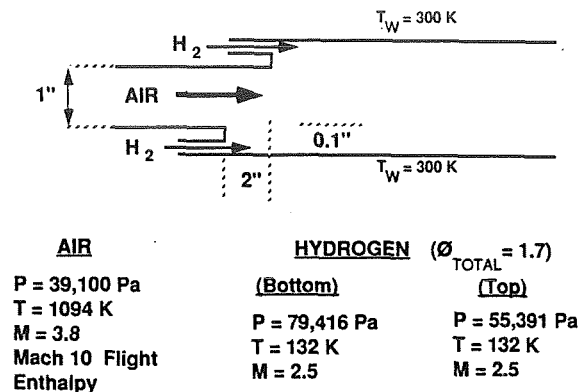
Figure 2. GASL/Calspan Run 41 Film Cooling Test Setup

percent on the top wall. The step on the top wall is 2 inches downstream of that on the bottom wall. Air at Mach 10 flight enthalpy enters the combustor with a 0.4 inch turbulent boundary layer on the bottom wall. Hydrogen is injected at Mach 2.5. The hydrogen and air mass flow rates are such that the equivalence ratio, defined as:

$$\varnothing = m_f/(m_a \times 0.0293) \quad \ldots \ldots \ldots \ldots \ldots (1)$$

where 0.0293 is the stoichiometric fuel-to-air mass flow rate ratio, is 1.7. Both walls are maintained at the fuel total temperature of 300 degrees K to represent a thermally balanced system.

The parabolic computation is started at the axial location of the bottom slot where the profiles of air velocity and temperature in the central 1 inch section of the duct are first specified. Pressure is assumed to be uniform and the vertical velocity is set to zero. Given the initial velocity profile, the turbulent kinetic energy, k and the dissipation rate, ε for the $k-\varepsilon$ turbulence model are initialized in the turbulent boundary layer according to the following rationale:

1. In a fully developed turbulent boundary layer, the generation and dissipation of turbulence are in balance. The transport equation for k then reduces to the following simple form [3]:

$$\tau = \rho \ kC_D^{1/2} \quad \ldots \ldots \ldots \ldots \ldots \ldots \ldots (2)$$

where C_D, one of the constants in the $k-\varepsilon$ model is equal to 0.09. The symbols τ and ρ are the density and the wall shear stress.

2. From the mixing length hypothesis,

$$\tau = \rho l^2_m (\partial w/\partial y)^2 \quad \ldots \ldots \ldots \ldots \ldots (3)$$

3. From turbulence measurements near walls [3], the variation of the mixing length in the boundary layer is known to be,

$$l_m = \kappa y, \text{ if } y < \lambda \delta/\kappa$$

$$= \lambda \delta, \text{ if } y > \lambda \delta/\kappa$$

or,

$$l_m(y) = min\ (\kappa y,\ \lambda \delta)\ \dots\dots\dots\ (4)$$

where δ is the boundary layer thickness, κ is one of the logarithmic law-of-the-wall constants (0.42) and λ has a value of 0.09.

4. The equation for the initial turbulent kinetic energy in the boundary layer is thus obtained by combining Equations (2), (3) and (4),

$$k = [min(\kappa y, \lambda \delta)/c_D^{1/4}\ \partial w/\partial y]^2\ \dots\dots\ (5)$$

Note that k is proportional to the square of the velocity gradient. Outside the boundary layer, k is set so that the freestream turbulence intensity k^2 is 0.05 percent.

5. The dissipation rate, ε is related to k and the turbulence length scale, l by definition as,

$$\varepsilon = c_D k^{3/2}/l\ \dots\dots\dots\dots\dots\dots\ (6)$$

where the length scale is related to the mixing length as,

$$l = c_D^{1/4} l_m\ \dots\dots\dots\dots\dots\dots\ (7)$$

Equation (6) along with (5), (7) and (4) are used to compute the initial profile of ε.

The flowfield at z=0.0 is thus completely specified on a grid that covers the central 1 inch portion of the duct. Before initiating space marching, the bottom boundary of the domain is extended downwards to accomodate the step. This extended domain is then regridded without changing the total number of grid points. The main flow is then conservatively patched onto the new grid as are the slot and lip flows. The same procedure is used at the second step. To suppress recirculation, the lip flow is given a small streamwise velocity (one percent of the freestream velocity), a pressure equal to the theoretical base pressure [4]
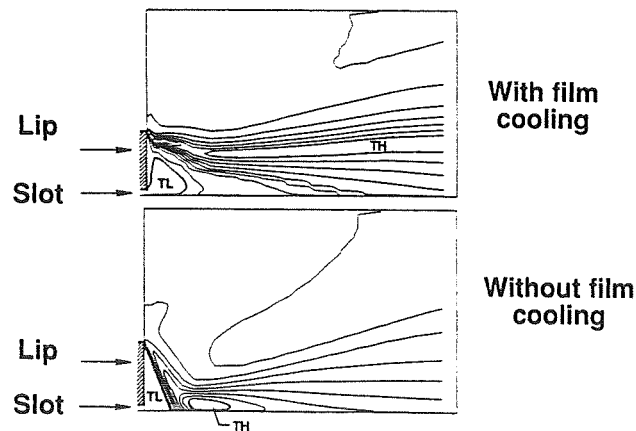

Figure 3.   Temperature Contours Near Slot From Parabolic Computation

and a temperature that is the average of the slot and lip temperatures. For cases without film cooling, the entire step is treated as a lip. The above treatment of the elliptic region at the lip causes little numerical difficulty because the pressure is treated so as to render the equations parabolic in the streamwise direction in subsonic regions [5]. Computed flowfields near the slot and lip region for a generic case with and without film cooling are shown in Figure 3, where the regions of high (freestream) and low (slot) temperatures are demarcated. The CPU time for the GASL-Calspan Run 41 analyzed here is 2 minutes on a Cray-2, using 81 grid points wall-to-wall and a minimum grid spacing of 10 microns at the walls.

The computed heat flux and pressure on the bottom wall are compared to the measured data in Figures 4 and 5. In this test, a sharp increase in the heat flux
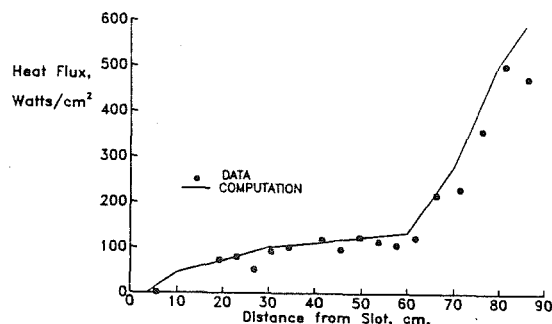

Figure 4. Comparison of Ship Computation vs Heat Flux Data
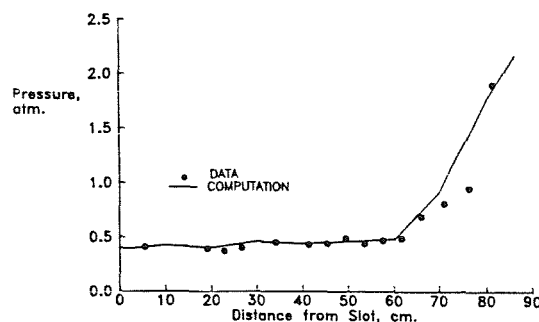

Figure 5. Comparison of SHIP Computation vs Pressure Data

at any location on the combustor walls is attributed largely to the degradation of the film by mixing and combustion, and not to shocks. This is because the test appraratus did not have strong shock generators such as fuel injectors or coverging walls. Thus, the rapid rise in both, heat flux and pressure data after 60 cm. indicates that ignition did not occur before 60 cm. The combustion downstream is not mixing-limited because, as seen from Figure 6, the computation shows an almost fully mixed condition at 60 cm. Thus, the finite slope of the rise in the heat flux and the pressure after 60 cm. must be attributed to kinetics, as is the ignition delay up to 60 cm. Lacking the capability to treat
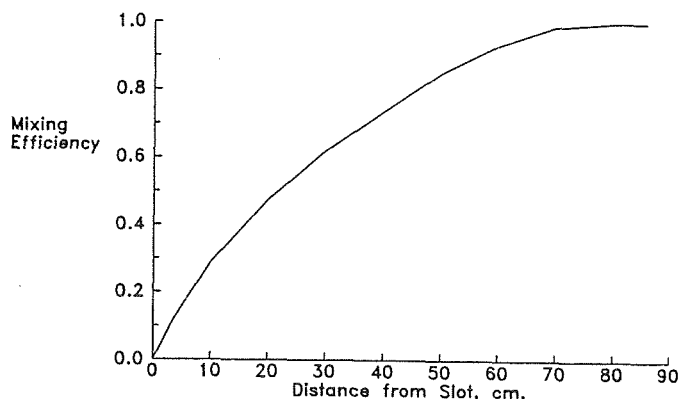

Figure 6. Mixing Efficiency Computed by SHIP

673

chemical kinetics in SHIP at present, the computation was performed assuming no reaction until 60 cm. downstream of which a non-kinetic, ramped reaction model was used. Thus, the predictive capability of SHIP for such relatively low enthalpy flows is, at present limited. However at the higher end of the hypersonic flight regime (Mach 16 to 25), where film cooling is expected to be used most, the assumption of mixing-limited combustion is quite valid and the existing capability is satisfactory.

TRANSVERSE INJECTION

In some supersonic combustor designs, fuel is injected transverse to the main flow to achieve a higher rate of mixing than parallel injection from a step. The flowfield in the vicinity of these injectors is elliptic due to the streamwise recirculation regions both upstream and downstream of injection. Parabolic treatment of transverse injection circumvents the need for an elliptic solution, which typically requires from 2 to 5 hours of CPU time on a Cray-class machine to solve just the region near a single injector. Such a procedure has recently been implemented in the SHIP3D code. In contrast to methods that use correlations or an equivalent body, the procedure involves the actual imposition of the injection boundary conditions during space-marching. Thus, it would allow the computation, not only of the combustion efficiency but also of the flow losses from which a performance parameter such as the combustor effectiveness can be obtained.

At present the procedure gives excellent mass conservation and good agreement with the mixing measurements, of Rogers [6]. The test setup and comparisons are shown in Figures 7 and 8. In that experiment, cold hydrogen was injected sonically through five injectors on a flat plate normal to a Mach 4
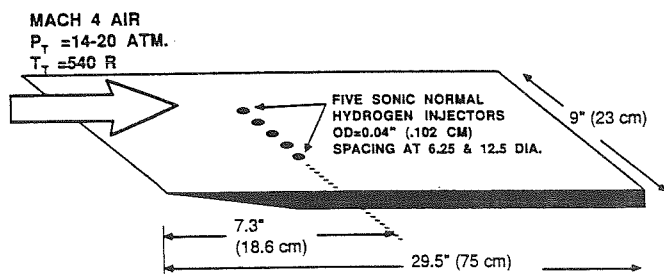

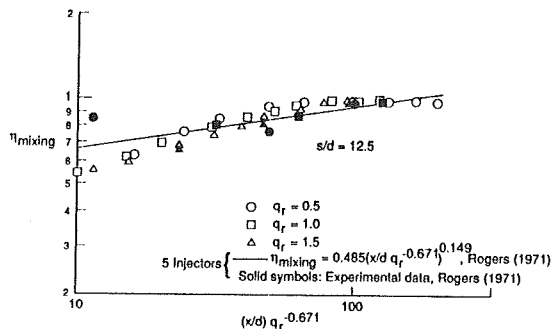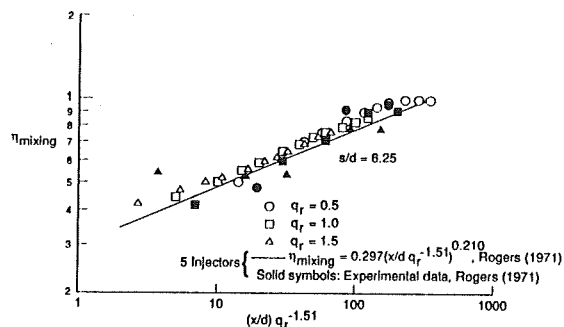Figure 7. Setup for Rogers Cold Flow Mixing Experiment

Figure 8. Parabolic Normal Injection vs Rogers Data

airstream. The dynamic pressure ratio was changed by varying the total pressure of the tunnel air and that of injection. Mass fraction surveys were conducted at distances up to 120 injector diameters downstream. These were integrated over the area fueled by the central injector to obtain the mixing efficiencies shown in Figure 8. For each case shown in Figure 8, the CPU time for a SHIP run using a 31 X 61 grid with a 100 micron minimum grid spacing is 3.5 minutes on a Cray-2. The standard values of the κ–ε model constants [5] were used in the computations. The domain covers the entire length of the flat plate and extends to the roof of the tunnel some 4.5 inches above the plate.

Although the predicted mixing efficiency is in agreement with data, the computed pressures downstream of the injector (not shown here) are high. Among the possible reasons for this behaviour, initialization of the flowfield upstream of injection, rather than the injection procedure itself, has been identified as the main cause. Validation using pitot pressure measurements close to the injectors is currently in progress.

PARAMETRIC ANALYSIS OF AN ACTIVELY COOLED SCRAMJET COMBUSTOR

Adequate cooling of the scramjet combustor walls at the upper end of the hypersonic flight regime is a critical design issue. It is estimated that a stoichiometric flow rate of the cryogenic hydrogen fuel is sufficient to regeneratively cool the engine upto a flight Mach number of 10. At higher speeds, film cooling and transpiration cooling are being considered to lower the wall heat load and thus, the fuel mass flow rate required for regenerative cooling. The analysis presented here covers both film and transpiration cooling in conjunction with regenerative cooling. One advantage of film cooling over transpiration cooling is that, at these high Mach numbers the streamwise momentum of the fuel makes a significant contribution to the thrust [7]. Both cooling methods however, degrade performance to some extent due to the poorer mixing and combustion associated with fuel injection close to the wall.
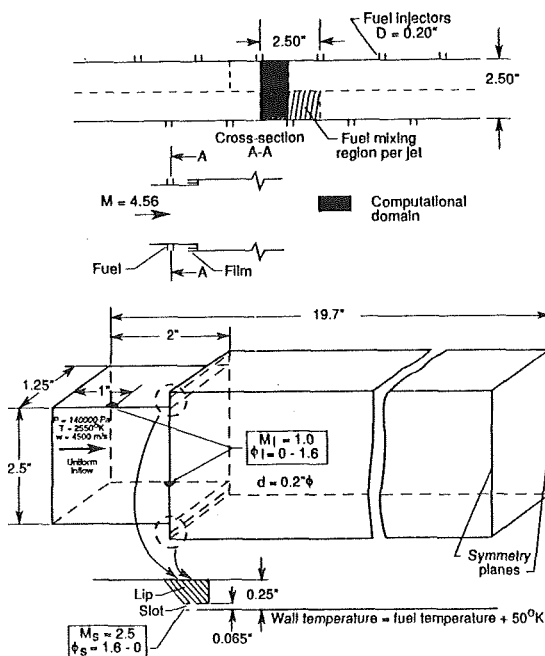
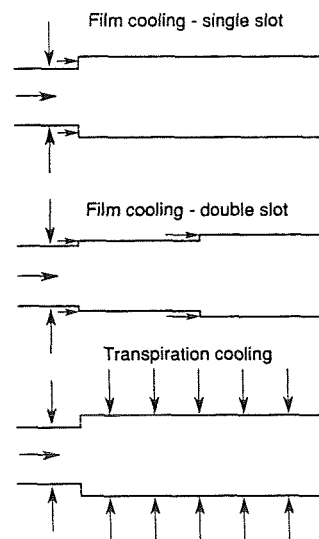Figure 9. Conceptual Combustor for Parametric Analysis

Figure 10. Combustor Configurations for Film Cooling and Transpiration Cooling
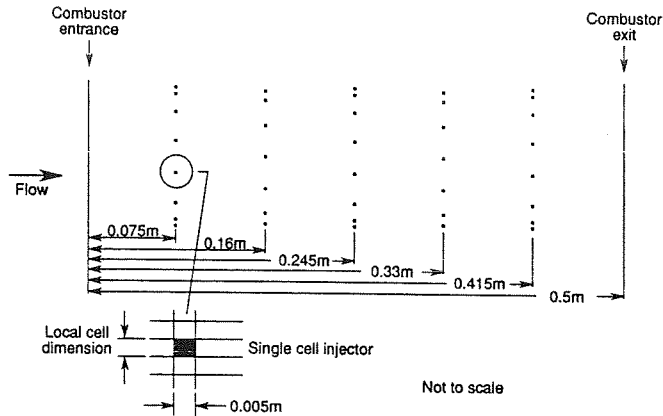
675

Figure 11.   Transpiration Cooling Injector Locations

     In this study, the relative magnitudes of these effects and the overall
influence on engine performance at Mach 16 flight is assessed on a hypothetical
vehicle with a conceptual combustor, shown in Figure 9.   The three cooling designs
in Figure 10, two using film cooling and one using transpiration cooling are
analyzed.   The transpiration cooling injector locations on each combustor wall are
shown in Figure 11. The porosity of the walls is chosen to be low solely to keep

the run times affordable.   The rest of the propulsion flowpath was specified in
sufficient detail for cycle analysis.   The parametric analysis involved a series
of three-dimensional, turbulent, reacting SHIP3D runs for the combustor with
different proportions of the fuel used for cooling while keeping the total fuel
and air flow rates constant.   Thus, the equivalence ratio, defined in Equation (1)
is kept constant at 1.6, a value considered typical at Mach 16 flight. The CPU
time for each film cooling run was 30 minutes on a Cray 2.   Each transpiration
cooling run however, required 5 hours because of transverse injection from each
cooling orifice into a finely resolved grid with a 5 micron grid spacing at the
walls.

     The computed quantities of interest are the longitudinal distribution of
mixing efficiency, wall heat flux and shear stress.   Using these results, the tip-
to-tail engine specific impulse is obtained using a cycle code. Additional details
of the methodology are given in reference [8].   In the following discussion, the
equivalence ratio is referred to as $\emptyset$. For the cases with high normal $\emptyset$, the
regions around the injectors and the steps are subject to severe heating due to
the glancing and impinging shocks from injectors on both walls.   Figure 12 shows
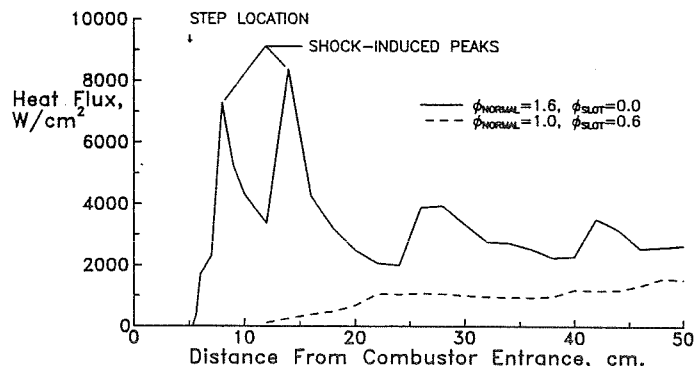

Figure 12.   Laterally-Averaged Heat Flux vs Distance

the laterally-averaged heat flux on the top wall, where the shock-induced peaks for the case without cooling are evident. For the case with a film cooling ⌀ of 0.6, both shock induced peaks are absent and the heat flux is generally lower.
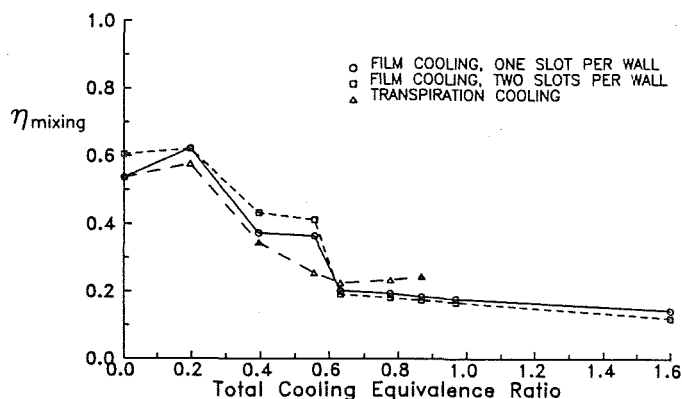

Figure 13. Mixing Efficiency at Combustor Exit

Figure 13 shows the variation in mixing efficiency at the combustion exit with the cooling ⌀. In this figure, an increase in the cooling ⌀ implies an equal decrease in the normal ⌀. For purely normal injection, the mixing efficiency is 0.537 while for a slot ⌀ of 0.2, it increases to 0.622. The latter is close to a fully mixed condition for this confined flow at a total ⌀ of 1.6. The reason for this unexpected increase in mixing with a decrease in the transverse ⌀ is that when all the fuel is injected normal to the flow, the fuel jets penetrate deep into the flow but do not adequately fuel the region near the wall. Thus, diversion of a small portion of the fuel to the slots improves mixing. For the same reason, the average wall heat flux at a cooling ⌀ of 0.2 is higher than that without cooling as shown in Figure 14. For the configuration with two film cooling slots
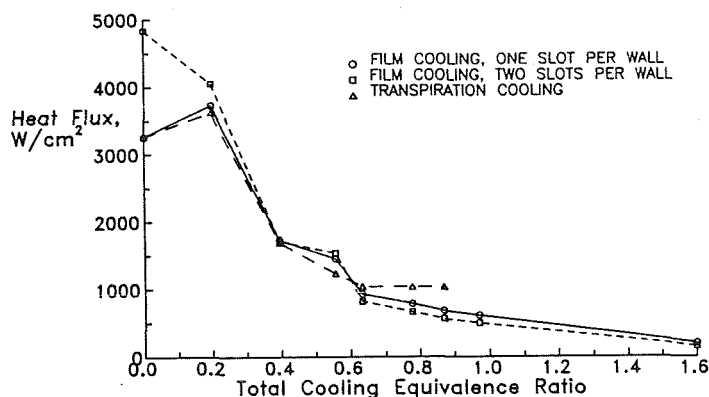

Figure 14. Average Combustor Wall Heat Flux

per wall, the higher average heat flux at low cooling ø is attributed to the higher average pressure in the combustor caused by the smaller steps.
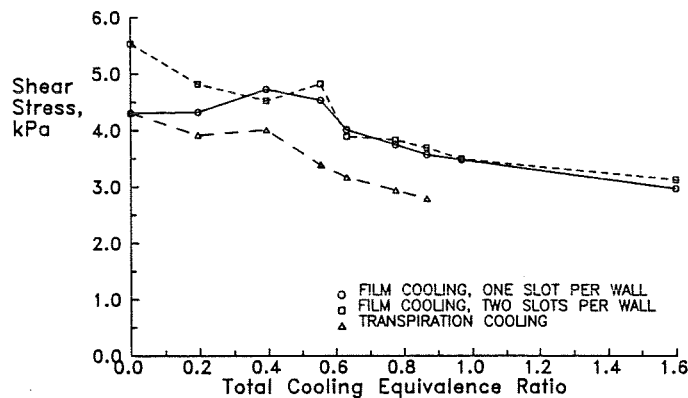

Figure 15. Average Wall Shear Stress

The average shear stress on the wall is shown in Figure 15. For film cooling, it follows the trend in the average heat flux (Figure 14) at only high cooling ø, where the behaviour is in agreement with Reynolds analogy. For transpiration cooling, the shear stress is consistently lower, indicative of the lower velocity gradients at the wall. Figures 13, 14 and 15 show that the greatest gain in cooling effectiveness is achieved when the cooling ø is increased from 0.2 to 0.6, with little change in wall shear, but accompanied by a drop in the mixing efficiency from 0.622 to 0.2. Not evident in these figures, however, is the contribution of the fuel momentum to thrust, which is the major advantage that film cooling has over transpiration cooling. For this, the results of cycle analysis are now examined.

The specific impulse, defined as the net thrust per unit fuel flow rate, is obtained from cycle analysis for each of the parametric SHIP3D combustor runs. The results, shown in Figure 16, indicate that the penalty in performance
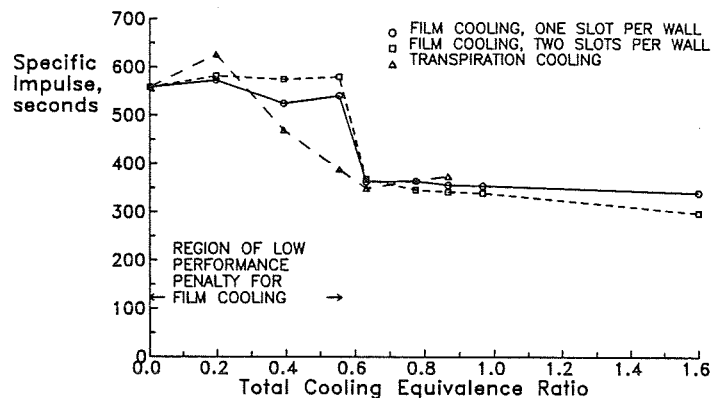

Figure 16. Tip-to-Tail Engine Specific Impulse

678

associated with film cooling is low for cooling ø up to 0.556, below which the contribution of the fuel momentum to thrust compensates for the drop in *mixing*. The balance is tipped at a film cooling ø of 0.556 above which the specific impulse drops sharply. This threshold value of the film cooling ø determines how effectively the combustor can be film cooled without a large penalty in performance.

For transpiration cooling, Figure 16 shows that this threshold value of the cooling ø is a low 0.2, at which the mixing efficiency also peaks (Figure 13). Since the momentum of the fuel used for transpiration cooling makes no contribution to the thrust, the specific impulse for transpiration cooling follows the decline in the mixing efficiency (Figure 13) with increasing cooling ø.

NOZZLES

Expansion of the combustor exhaust against the lower rear portion of the fuselage, which serves as a nozzle, is the main thrust generating mechanism in an airframe-integrated scramjet. Thus the nozzle problem requires the computation of the pressure on the entire, contoured nozzle wall. Figure 17 shows the sideview
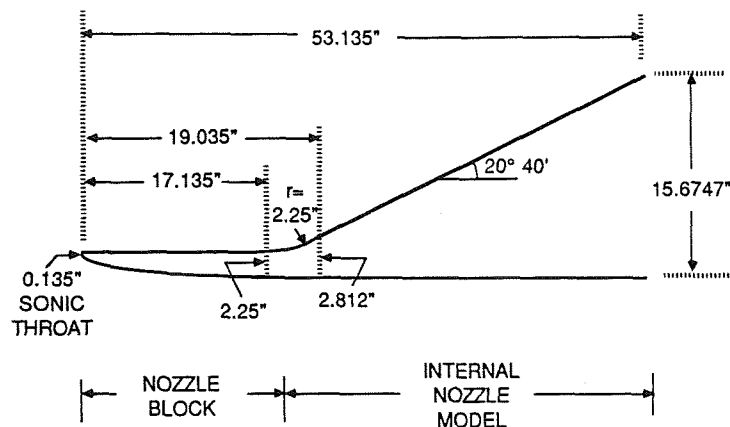

Figure 17. Sideview of Nozzle Block and Internal Nozzle Model

of a nozle that was tested using high pressure air [9]. The nozzle block sets up a Mach 4-5 flow, which simulates a scramjet combustor exhaust at Mach 20-25 flight. This flow is then expanded in the internal nozzle model, the bottom wall of which represents a cowl. Measurements of wall pressure and heat flux, the overall thrust and boundary layer surveys were taken to provide data to validate codes for the two key nozzle unit problems, expansion and boundary layer development.

The parabolic computation of this air-only case was run from the sonic throat all the way to the exit. Forty-one grid points are used from wall-to-wall and the minimum grid spacing at the throat is 30 microns. The grid is expanded proportionately to the expansion of the duct as the computation proceeds downstream. The CPU time for this case is 4 minutes on a Cray-2.

The computed and measured pressures are compared in Figures 18 and 19 for the nozzle block and internal nozzle model. The increase in the computed lower wall pressure between 0.3 and 0.43 m is slightly in excess of that shown by the data. For the top wall of the internal nozzle (Figure 19), the computation and
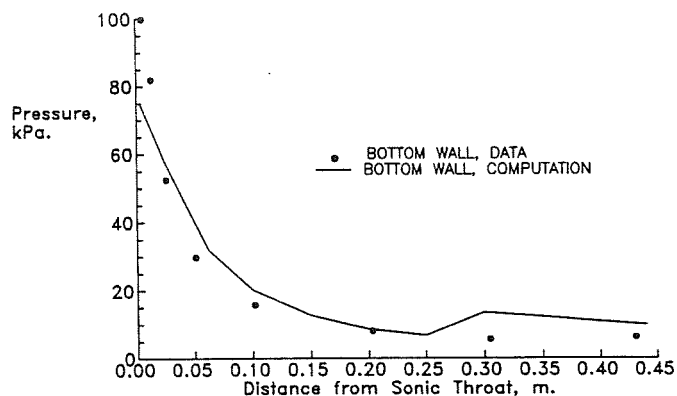
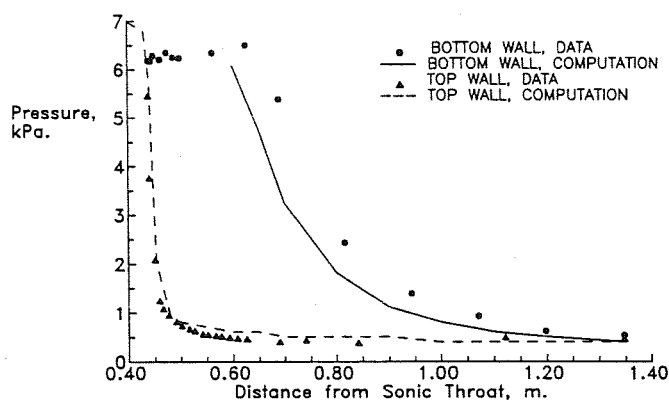**Figure 18. Wall Pressure for Nozzle Block**

Figure 19. Wall Pressure for Internal Nozzle Model

test data are in good agreement.   For this wall, the computed thrust is higher than that obtained by integrating the measured presures by 4.3 percent.

Because of the quasi-orthogonal metrics used in SHIP [5], a sudden change in the slope of the wall causes some locally oscillatory behaviour in the pressure which however, quickly recovers to the correct value. Work on a more realistic coordinate transformation is currently in progress.

SUMMARY

The SIMPLE-based three-dimensional parabolic flow code, SHIP3D is shown to be a highly efficient code for scramjet combustor and nozzle computations.   The capability to accurately compute the heat transfer in a turbulent, reacting

flowfield makes it particularly suitable for combustor film cooling studies. This along with recently implemented methods for the parabolic treatment of fuel injection, makes it possible to conduct parametric studies of realistic combustor configurations. One such study is included in this paper.

A simulated scramjet nozzle flow at flight Mach 20 to 25 is computed. For this preliminary analysis, the agreement with the pressure force, obtained by integration of the measured pressures, is within 4.3 percent.

For those computations not involving heat transfer, where a minimum grid spacing of the order of 50 to 100 microns suffices, 1 to 5 CPU minutes is the typical run time on a Cray-2. The memory required is usually less than 1 million words. Thus, the SHIP code could be run productively on a machine as small as a personal computer.

REFERENCES

1. Northam, G. B. and Anderson, G. Y.: "Supersonic Combustion Ramjet Research at Langley," AIAA Paper No. 86-0159, 1986.

2. Srinivasan, S., McClinton, C. R. and Kamath, P. S.: "Numerical Simulation of Flow Through the Langley Parametric Scramjet," SAE Paper 892314, Aerospace Technology Conference and Exposition, Anaheim, California, September 25-28, 1989.

3. Ng, K. H. and Spalding, D. B.: "Turbulence Model for Boundary Layers Near Walls," The Physics of Fluids, v15, n1, pp 20-30, January 1972.

4. Love, E. S.: "Base Pressure at Supersonic Speeds on Two-dimensional Airfoils and on Bodies of Revolution With and Without Fins Having Turbulent Boundary Layers," NACA TN-3819, 1957 (supersedes NACA RM L53C02).

5. Markatos, N. C., Spalding, D. B. and Tatchell, D. G.: "Combustion of Hydrogen Injected into a Supersonic Airstream (The SHIP Computer Program)," NASA CR-2802, April 1977.

6. Rogers, R.C.: "Mixing of Hydrogen Injected from Multiple Injectors Normal to a Supersonic Airstream," NASA TN-D-6476, 1971.

7. Kamath, P.S., Baker, N.R. and McCLinton, C. R,: "Film Cooling vs Transpiration Cooling for Scramjet Combustors - A Computational Study," Paper No. 96, Seventh NASP Technology Symposium, October 23-27, 1989.

8. Kamath, P.S., Baker, N. R., and McClinton, C. R.: "A Computational Design Tool for Scramjet Combustor Film Cooling and Fuel Mixing Predictions, AIAA Paper No. 90-0645.

9. Seifertt, T.:"Generic Option No. 2 Validation/Experimental Database Development Hypersonic Nozzle Test Program," Paper No. 85, Seventh NASP Technology Symposium, October 23-27, 1989.